Scripta Materialia 112 (2016) 62–66

Contents lists available at ScienceDirect

Scripta Materialia

journal homepage: www.elsevier.com/locate/scriptamat

Tunable dielectric properties induced by optical fields in barium strontium titanate/manganite heterostructures

K.X. Jin *, B. Yang, Y. Zhang, B.C. Luo, L.Y. Chen, C.L. Chen

Shaanxi Key Laboratory of Condensed Matter Structures and Properties, School of Science, Northwestern Polytechnical University, Xi'an 710072, China

ARTICLE INFO

Article history:
Received 24 July 2015
Received in revised form 7 September 2015
Accepted 7 September 2015
Available online 18 September 2015

Keywords:
Heterostructures
Dielectric
Electrical properties
Ferroelectricity

ABSTRACT

We systematically investigated the microstructure, leakage current, and tunability of dielectric constants in barium strontium titanate/manganite heterostructures induced by optical fields. It is interesting to note that the values of the relative variation in the dielectric constants have a transition from positive to negative at 150 K when the heterostructure is irradiated by the optical field. This might be attributed to the effect of photogenerated carriers at different structural phases of the barium strontium titanate. These results provide a further understanding of the optical-electric coupling effect and potential applications for tunable microelectronic devices.

1. Introduction

Barium strontium titanate $Ba_xSr_{1-x}TiO_3$ thin films have become extremely attractive for applications in the next generation microwave tunable devices and dynamic random access memories [1–5]. Thus, it has spurred fundamental studies in modulating electrical properties to satisfy requirements absolutely of these devices with relatively high dielectric constant and low dielectric loss. Generally, the electrical properties can be modified by the grain boundaries [6], the interface engineering [7–9], the compositional design (*e.g.* donor doping) [10–12], the stress [13,14] and so on [15,16]. Meanwhile, the external fields, such as electric and optical fields, could also modulate the dielectric and ferroelectric properties of films effectively. For examples, the optical fields would produce the current and the ferroelectric photovoltaic effect in dielectrics [17–19]. The applied voltages can result in nonlinear behaviors in the dielectric properties of $Ba_xSr_{1-x}TiO_3$ materials [20]. As ferroelectric materials, the integration with other functional materials (*e.g.* magnetic materials) can give rise to emergent properties and potential applications [21–23]. Furthermore, some research studies have indicated that the $La_{0.67}Sr_{0.33}MnO_3$ (LSMO) possesses low resistivity, excellent thermal stability, good adhesion to films, and further conducts as a functional element due to its ferromagnetism [24]. So the LSMO becomes the optimum selection of bottom electrodes for $Ba_xSr_{1-x}TiO_3$ films in comparison with other perovskite conductive oxides [25,26]. In the past years, heterostructures, composed of ferroelectric and ferromagnetic layers, have attracted more attention due to multiferroics as promising candidates for data storages and sensors [27–31]. Especially, there are many investigations on ferroelectric and dielectric properties of $Ba_xSr_{1-x}TiO_3$/LSMO heterostructures [32–35]. Traditionally, the magnetic-electric couplings are focused in these heterostructures. On the other hand, the photoinduced effect, being the external perturbation of heterostructures, provides a handy and reliable method to induce the change of properties and rewritable optical media [36,37]. Moreover, the modulations of dielectric response induced by the optical fields and the optical-electric couplings are very limited although some photoinduced effects are observed as well [17–19]. Therefore, the perovskite oxide $Ba_{0.6}Sr_{0.4}TiO_3$ (BST)/LSMO heterostructures were fabricated by a pulsed laser deposition method in this work. We investigate the microstructure, surface morphology, and ferroelectric properties of the films. Moreover, the dielectric responses of the heterostructure irradiated by the optical field ($\lambda = 532$ nm) are systemically discussed.

2. Experimental details

The LSMO and BST films were successively deposited *in situ* on a (001) $LaAlO_3$ (LAO) substrate using a pulsed laser deposition method. The conditions for depositing the LSMO layer are as follows: the laser with a wavelength of 248 nm, a repetition rate of 2 Hz, the pulse energy of approximately 145 mJ. The substrate temperature was kept at 850 °C and an oxygen pressure of 5 Pa was maintained throughout the deposition. After deposition, the LSMO layer was annealed at 850 °C for 60 min in oxygen with the pressure of 300 Pa. The BST layer was then deposited *in situ* on the top of the LSMO layer at 750 °C with an oxygen pressure of 10 Pa. A laser energy of 145 mJ and a repetition rate of 3 Hz were used. After deposition, the as-deposited heterostructure was annealed *in situ* at 750 °C at a dynamic oxygen

* Corresponding author.
E-mail address: jinkx@nwpu.edu.cn (K.X. Jin).

http://dx.doi.org/10.1016/j.scriptamat.2015.09.012
1359-6462/

pressure of 300 Pa for 60 min and was then cooled down to room temperature slowly. The BST/LSMO heterostructure were analyzed with an X-ray diffractometer (RigakuD/max2200) using Cu Kα radiation. The surface topography was illustrated by an Asylum Research MFP-3DTM atomic force microscopy (AFM) in the tapping mode. The surface and cross section morphologies of the heterostructures were observed using a field-emission scanning electron microscope (SEM, Quanta 600FEG, America FEI). Square top platinum electrodes with a side length of 0.5 mm were sputtered by a sputtering instrument through a shadow mask. The current–voltage curves of the heterostructure were obtained using a current (DC) voltage source (Keithley 6487). The ferroelectric properties of the BST layer were characterized using a commercial ferroelectric tester (Precision LC, Radiant Technologies). The dielectric properties of the heterostructure irradiated by the optical field were measured using a LCR meter in the temperature range from 50 K to 300 K. During the measuring process, our samples were placed in a Janis CCS300 closed circuit cryostat with quartz glass windows. And due to the continuous cooling of the samples, the heating effect can be neglected.

3. Results and discussion

Fig. 1(a) shows the typical x-ray diffraction θ–2θ scan pattern of the BST/LSMO heterostructure. Only the (00 l) peaks of BST and LSMO films are observed, indicating that both the BST and LSMO layers have a c-axis orientation. The BST film is under a compressive stress in the plane and the lattice mismatch is about 2.6%. The insets show the surface morphologies of BST and LSMO layers obtained by AFM. The values of the root-mean-square roughness for the BST and LSMO layers are about 1.66 and 1.23 nm, respectively. Fig. 1(b) shows the SEM photograph of the BST film surface, demonstrating the BST film is comparatively homogeneous and the grains boundaries with the average size of about 50 nm are clear. Moreover, the cross-sectional SEM image of the heterostructure is shown in Fig. 1(c). The thicknesses of the LSMO and BST layers are, respectively, about 320 and 460 nm. It also can be seen that the heterostructure exhibits sharp interfaces, indicating that there is less chemical action or atomic diffusion between the interfaces.

Fig. 2(a) shows the hysteresis curves of BST/LSMO heterostructure at different applied voltages. The inset shows the sketch of the configuration of ferroelectric capacitor. The evident hysteresis loop indicates that the BST/LSMO heterostructure presents good ferroelectric properties at room temperature. Meanwhile, a small operating voltage (~3 V) could make the polarization reversible. The values of spontaneous polarization (P_s) and remanent polarization (P_r) increase with increasing applied voltages. The measured maximum values of P_s and P_r are 13.9 and 2.15 μc/cm^2 at the applied voltage of 30 V, respectively.

To analyze the leakage current mechanisms of our sample, we present the log–log plot of the leakage current at positive biases for the BST/LSMO heterostructure as shown in Fig. 2(b). The curves can be divided into two distinct regions according to the slope values. In the region *A*, the curves show a roughly linear dependence at the measured temperature range and all the slopes are near to unity, indicating that the Ohmic contact dominates the leakage characteristics. Furthermore, the slope values are less than 1 in the region *A* due to the insufficient charging time to reach the steady conduction current while the test is performed [38]. As the bias voltages increase, the curves get into another linear region (*B*) and the slope values are increased from 2.7 to 4.2 with increasing the temperatures from 50 to 300 K. The curves fitted using Schottky and Poole–Frenkel emission model aren't well consistent with the experimental data. So, the trap-filling progress of

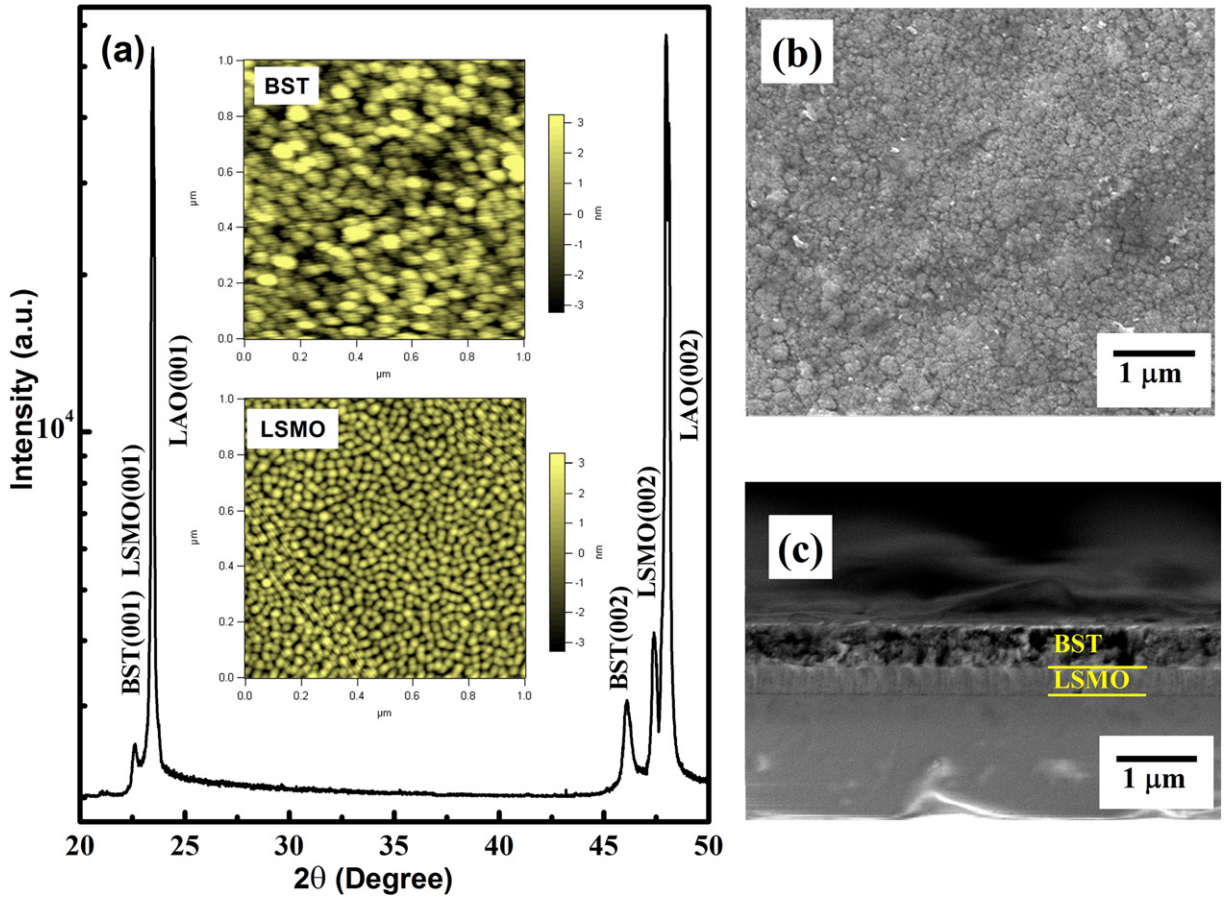

Fig. 1. (a) X-ray diffraction θ–2θ scan pattern of the BST/LSMO heterostructure deposited on the $LaAlO_3$ substrate. The insets show the AFM surface morphologies of BST and LSMO layers. (b) FE-SEM surface photograph of BST thin film (scale bar—2 μm). (c) FE-SEM cross-section photograph of the heterostructure (scale bar—2 μm).